THE JOURNAL OF BIOLOGICAL CHEMISTRY
Vol. 279, No. 42, Issue of October 15, pp. 43769–43779, 2004
Printed in U.S.A.

Synapsin Is a Novel Rab3 Effector Protein on Small Synaptic Vesicles

II. FUNCTIONAL EFFECTS OF THE Rab3A-SYNAPSIN I INTERACTION*

Received for publication, April 14, 2004, and in revised form, July 8, 2004
Published, JBC Papers in Press, July 20, 2004, DOI 10.1074/jbc.M404168200

Silvia Giovedì‡, François Darchen§, Flavia Valtorta¶, Paul Greengard‖, and Fabio Benfenati‡‖**

From the ‡Department of Experimental Medicine, Section of Human Physiology, University of Genova, Via Benedetto XV, 16132 Genova, Italy, §CNRS UPR 1929, Institut de Biologie Physico-Chimique, 13 Rue Pierre et Marie Curie, F-75005 Paris, France, the ¶Department of Neuroscience, S. Raffaele Vita-Salute University, Via Olgettina 58, 20132 Milano, Italy, and ‖Laboratory of Molecular and Cellular Neuroscience, The Rockefeller University, New York, New York 10021-6399

Synapsins, a family of neuron-specific phosphoproteins that play an important role in the regulation of synaptic vesicle trafficking and neurotransmitter release, were recently demonstrated to interact with the synaptic vesicle-associated small G protein Rab3A within nerve terminals (Giovedì, S., Vaccaro, P., Valtorta, F., Darchen, F., Greengard, P., Cesareni, G., and Benfenati, F. (2004) *J. Biol. Chem.* 279, 43760–43768). We have analyzed the functional consequences of this interaction on the biological activities of both proteins and on their subcellular distribution within nerve terminals. The presence of synapsin I stimulated GTP binding and GTPase activity of both purified and endogenous synaptic vesicle-associated Rab3A. Conversely, Rab3A inhibited synapsin I binding to F-actin, as well as synapsin-induced actin bundling and vesicle clustering. Moreover, the amount of Rab3A associated with synaptic vesicles was decreased in synapsin knockout mice, and the presence of synapsin I prevented RabGDI-induced Rab3A dissociation from synaptic vesicles. The results indicate that an interaction between synapsin I and Rab3A exists on synaptic vesicles that modulates the functional properties of both proteins. Given the well recognized importance of both synapsins and Rab3A in synaptic vesicles exocytosis, this interaction is likely to play a major role in the modulation of neurotransmitter release.

Rab proteins, belonging to the Ras superfamily of small G proteins, are implicated in the regulation of membrane trafficking between subcellular compartments (1, 2). Rab3A–C are expressed in brain where they specifically associate with synaptic vesicles (SV)[1] (3). Rab3A, the most abundant and widely distributed isoform in brain, cycles between a GTP-bound form that associates with the SV membrane and a GDP-bound form that becomes soluble upon formation of a complex with the GDP dissociation inhibitor (RabGDI) (for review see Refs. 2, 4, and 5). The cycling of Rab proteins is strictly linked to the exo-endocytotic cycle of SV. Stimulation of neurotransmitter release promotes GTP hydrolysis and dissociation of Rab3A from the SV membrane (6, 7), whereas overexpression of GTPase-deficient, constitutively active Rab3A inhibits neurotransmitter release (8–10).

Rab3 has been proposed to regulate vectorially SV trafficking at various stages of the exo-endocytotic cycle through interactions with specific effector proteins. Rab3 may participate in the docking of SV to appropriate sites of the presynaptic membrane by interacting with presynaptic effectors localized at active zones, such as Rim (11), as well as in the following priming and fusion events by interacting with a prefusion complex and preventing fusion of primed SV with the presynaptic membrane (for review see Refs. 4, 5, and 12). Whereas most of the hypothesized roles of Rab3A has been confirmed by studies on Rab3A knockout mice (13), its role in docking has been questioned, as Rim knockout mice do not exhibit changes in the number of docked SV (14). Under conditions of high frequency stimulation, Rab3A knockout mice exhibit a decrease in the recruitment of SV at the presynaptic membrane and a delayed recovery of release after stimulation (15), whereas train and paired-pulse facilitations were increased after injection of constitutively active Rab3A into *Aplysia* neurons (10). These effects, together with the described interaction between the Rab3 effector Rabphilin-3 and the actin bundling protein α-actinin (16), implicate Rab3 in the activity-dependent trafficking of SV upstream of SV fusion, possibly by affecting the dynamics of SV binding to the actin cytoskeleton.

After endocytosis of the fused SV, soluble Rab3A dissociates from RabGDI, reassociates with the SV membrane, and undergoes a GDP/GTP exchange that involves the intervention of a guanine nucleotide-exchange factor. It has been demonstrated recently that GTP/GDP exchange is not a prerequisite for Rab3A binding to the SV membrane and that GDP-bound Rab3A binds to a protein component of SV that competes with

* This work was supported by Italian Ministry of University Grants Cofin 2001, 2002, 2003, and FIRB (to F. B. and F. V.), Fisher Foundation for Alzheimer's Disease Research (to F. B.), CNR (Progetto Strategico Neuroscienze and Genomica Funzionale (to F. B. and F. V.), United States Public Health Service Grants MH39327 and AG15072 (to P. G.), and Telethon-Italy Grant 1131 (to F. B.). The costs of publication of this article were defrayed in part by the payment of page charges. This article must therefore be hereby marked "*advertisement*" in accordance with 18 U.S.C. Section 1734 solely to indicate this fact.

** To whom correspondence should be addressed: Dept. of Experimental Medicine, Section of Human Physiology, University of Genova, Via Benedetto XV, 3, 16132 Genova, Italy. Tel.: 39-10-3538183; Fax: 39-10-3538194; E-mail: benfenat@unige.it.

[1] The abbreviations used are: SV, synaptic vesicles; BSA, bovine serum albumin; CaMKII, Ca^{2+}/calmodulin-dependent protein kinase type II; cdk-1, cyclin-dependent protein kinase; DTT, dithiothreitol; FRET, fluorescence resonance energy transfer; GAP, GTPase-activating protein; GDI, GDP dissociation inhibitor; GST, glutathione *S*-transferase; LRh-PE, *N*-[lissamine rhodamine B sulfonyl] L-α-phosphatidylethanolamine; MAPK, mitogen-associated protein kinase Erk 1/2; NBD-PE, *N*-[4-nitrobenzo-2-oxa-1,3-diazole] L-α-phosphatidylethanolamine; PC, phosphatidylcholine; PE, phosphatidylethanolamine; PI, phosphatidylinositol; PS, phosphatidylserine; PKA, cAMP-dependent protein kinase; RSV, synapsin-rebound synaptic vesicles; SSV, synapsin-depleted synaptic vesicles; USV, untreated synaptic vesicles; GTPγS, guanosine 5′-3-*O*-(thio)triphosphate.

soluble RabGDI for Rab3A delivery (17, 18). A GDI dissociation factor has been identified recently for Rab5 and Rab9 (19, 20), and a similar factor could be involved in the translocation of GDP-Rab to SV.

As Rab3 represents a clock for exocytosis, the identification of Rab3 partners that modulate its cycle may be important for the understanding of the fine mechanisms of neurotransmitter release. By using phage display library analysis to uncover high affinity synapsin-binding peptides, we have recently found that Rab3A is one of the synapsin interactors in intact nerve terminals (62).

Synapsins, a family of neuron-specific phosphoproteins, have been demonstrated to regulate the supply of SV available for exocytosis by binding to both SV and actin cytoskeleton in a phosphorylation-dependent manner (for review see Refs. 21 and 22). Although these observations strongly support a predocking role of the synapsins in the assembly and maintenance of a large reserve pool of SV and in the regulation of short term synaptic plasticity, recent results indicate that the synapsins are also involved in some later step of exocytosis. Thus, the kinetics of release was slowed in the squid giant terminal after injection of a conserved synapsin COOH-terminal peptide (23), as well as in *Aplysia* ganglion neuron terminals after neutralization of endogenous synapsin by antibody injection (24).

As synapsins act as regulators of SV trafficking at both pre- and post-docking stages of the SV cycle, we studied whether the synapsin-Rab3 interaction plays some role in the multiple stages of exocytosis. In this paper, we demonstrate that the interaction between synapsin and Rab3A regulates the activities of both proteins. Thus, synapsin stimulated the Rab3A cycle by increasing GTP binding, GTPase activity, and Rab3A recruitment to the SV membrane, and conversely, Rab3A inhibited the actin binding and SV clustering activity of synapsin.

EXPERIMENTAL PROCEDURES

Materials

[α-^{32}P]GTP, [γ-^{32}P]GTP, γ-^{35}S-GTP, [^{3}H]GDP, and glutathione-Sepharose were from Amersham Biosciences. Human recombinant Rab3A was from Calbiochem; Bio-Spin 6 gel filtration columns were from Bio-Rad; PEI-cellulose TLC sheets were from Merck; nitrocellulose membranes and 0.45-μm filters were from Schleicher & Schuell; the Renaissance enhanced chemiluminescence detection system was from PerkinElmer Life Sciences. The anti-synapsin and anti-Rab3A polyclonal antibodies were raised in our laboratories. The other antibodies were obtained from available commercial sources. Rat RabGDI was expressed as His_6-tagged protein in BL21(DE3) pLysS strain and purified to homogeneity on nickel-nitrilotriacetic acid-agarose affinity columns (Qiagen, Valencia, CA). Purified bovine synapsin I was stoichiometrically phosphorylated *in vitro* by using purified protein kinase A (PKA), Ca^{2+}/calmodulin-dependent protein kinase type II (CaMKII), mitogen-associated protein kinase Erk 1/2 (MAPK), or cyclin-dependent protein kinase-1 (cdk-1) as described previously (25, 26). Bovine brain phosphatidylcholine (PC), bovine brain phosphatidylethanolamine (PE), bovine brain phosphatidylserine (PS), bovine liver phosphatidylinositol (PI), *N*-[4-nitrobenzo-2-oxa-1,3-diazole]-L-α-phosphatidylethanolamine (NBD-PE), and *N*-(lissamine rhodamine B sulfonyl)-L-α-phosphatidylethanolamine (LRh-PE) were obtained from Avanti Polar Lipids (Alabaster, AL), stored at −20 °C in the dark, and used within 3 months. Bovine serum albumin (BSA) and all other chemicals were from Sigma. SV were purified to homogeneity from rat forebrain through the step of controlled pore glass chromatography (27). Mouse forebrain homogenate was subfractionated through the step of sucrose density gradient centrifugation as described (27) yielding purified SV and synaptic membrane fractions (SG2 and SG4 fractions, respectively).

Assays of the Biochemical Properties of Rab3A

Binding of γ-^{35}S-GTP to Rab3A—The binding of γ-^{35}S-GTP to Rab3A was evaluated as described by Kikuchi *et al.* (28) with some modifications. Recombinant Rab3A was loaded with GDP (1 μM) by incubation for 20 min at 30 °C in loading buffer (20 mM Tris-Cl, 25 mM NaCl, 4 mM EDTA) containing 1 mM dithiothreitol (DTT), and the nucleotide-protein complex was stabilized by chilling the samples on ice and adding $MgCl_2$ to a final concentration of 20 mM. GDP-loaded Rab3A (2 pmol/sample; final volume 50 μl) was then incubated with increasing concentrations (30–1000 nM) of γ-^{35}S-GTP for 15 min at 30 °C in binding buffer (20 mM Tris-Cl, 10 mM EDTA, 5 mM $MgCl_2$, 1 mM DTT, pH 7.5) in the absence or presence of synapsin I (1 μM). Nonspecific binding was defined as the binding in the presence of an excess unlabeled GTP (300 μM). The reaction was stopped by the addition of 2 ml of ice-cold stopping solution (25 mM Tris-Cl, 20 mM $MgCl_2$, 100 mM NaCl, pH 7.4) followed by rapid filtration on 0.45-μm nitrocellulose filters. Filters were washed five times with ice-cold stopping solution, and the retained radioactivity was determined by liquid scintillation counting. For the analysis of GTP binding to SV, synapsin-depleted SV (SSV) were first loaded with GDP (500 μM) as described above, and the excess GDP was removed by high speed centrifugation (400,000 × *g* for 20 min) after addition of 20 mM $MgCl_2$ (17). GDP-loaded SV (10 μg of protein/sample) were assayed for γ-^{35}S-GTP binding as described above, followed by filtration and scintillation counting.

Dissociation of [^{3}H]GDP from Rab3A—Recombinant Rab3A or SSV were loaded with [^{3}H]GDP (1 μM) by incubation at 30 °C for 20 min in 20 mM Tris-Cl, 4 mM EDTA, 1 mM DTT, pH 7.4, followed by cooling the samples on ice and adding $MgCl_2$ to a final concentration of 20 mM. The dissociation of [^{3}H]GDP from recombinant Rab3A (2 pmol/sample) or SSV (10 μg protein/sample) was initiated at time $t = 0$ by the addition of a 200-fold excess of unlabeled GTP in a mixture containing 20 mM Tris-Cl, 200 mM NaCl, 2 mM $MgCl_2$, 1 mM DTT, pH 7.5, in the absence or presence of synapsin I (1 μM). The reaction was stopped by filtration on 0.45-μm nitrocellulose filters as described above at various times (15 min to 3 h) after the addition of GTP (28).

Rab3A GTPase Activity—Assays for Rab3A GTPase activity were performed as described previously (28, 29) with some modifications. For the formation of the [α-^{32}P]GTP-Rab3A complex, recombinant Rab3A (25 pmol/sample) or purified SV (5 μg of protein/sample) were incubated for 10 min at 30 °C in loading buffer containing 50 nM [α-^{32}P]GTP (1 μCi/sample). The mixture was placed on ice, and $MgCl_2$ was added to a final concentration of 20 mM to stabilize the nucleotide-protein complex. Excess unbound [α-^{32}P]GTP was removed by passage through a gel filtration column Bio-Spin 6, previously equilibrated in reaction buffer (20 mM Tris-Cl, pH 7.4, 100 mM NaCl, 5 mM $MgCl_2$, 1 mM DTT). For the measurement of GTPase activity, GTP-loaded samples were incubated at 30 °C in reaction buffer in the absence or presence of purified synapsin I (25 pmol/sample). Aliquots (20 μl) of the reaction mixtures were taken at various time intervals and stopped by the addition of 0.2% (w/v) SDS, 2 mM DTT, 2 mM EDTA, 0.5 mM GTP, 0.5 mM GDP (final concentration) followed by incubation at 65 °C for 20 min. The ratio of GTP and GDP bound to Rab3A was quantified by TLC as described previously (30). Aliquots were applied to PEI-cellulose TLC sheets, which were then immersed in methanol for 5 min, dried at room temperature, and developed with 4 M formic acid (brought to pH 3.5 with NH_4OH). After completion of the run (about 1 h), chromatograms were immersed in methanol for 20 min, dried, and exposed at −80 °C. Based on nucleotide staining, the radioactive spots corresponding to [α-^{32}P]GTP and [α-^{32}P]GDP were scraped from the chromatogram and counted by liquid scintillation spectrometry. The hydrolysis of Rab3A-bound GTP was expressed as percent increase in [α-^{32}P]GDP formation with respect to the amount of [α-^{32}P]GDP present at time 0.

Rab3A-GTPase Activating Protein (GAP) Activity—Recombinant Rab3A (10 pmol/sample), loaded with [γ-^{32}P]GTP as described above, was incubated with recombinant Rab3-GAP for 6 min at 25 °C in the absence or presence of either Rabphilin-3 or synapsin I in a buffer containing 20 mM Tris-Cl, 100 mM NaCl, 1 mM $MgCl_2$, pH 8.0. At the end of the incubation, samples were diluted with ice-cold buffer and filtered through 0.45-μm nitrocellulose membranes, and the retained radioactivity was determined by scintillation counting (31).

Assays of the Biochemical Properties of Synapsin I

Actin Binding and Bundling Assays—G-actin (5 μM) purified as described previously (32) in G-buffer (0.2 mM ATP, 0.2 mM $CaCl_2$, 0.5 mM 2-mercaptoethanol, 0.5 mM NaN_3, 2 mM Tris-Cl, pH 8.0) was polymerized for 1 h at room temperature by the addition of 90 mM KCl, 2 mM $MgCl_2$ and incubated at 25 °C for 1 h with synapsin I (0.5 μM), Rab3A (0.5–5 μM), or synapsin I plus Rab3A in the presence of either GTPγS or GDP. Identical samples were centrifuged either at low speed (10,000 × *g* for 10 min) for recovery of actin bundles or subjected to high speed

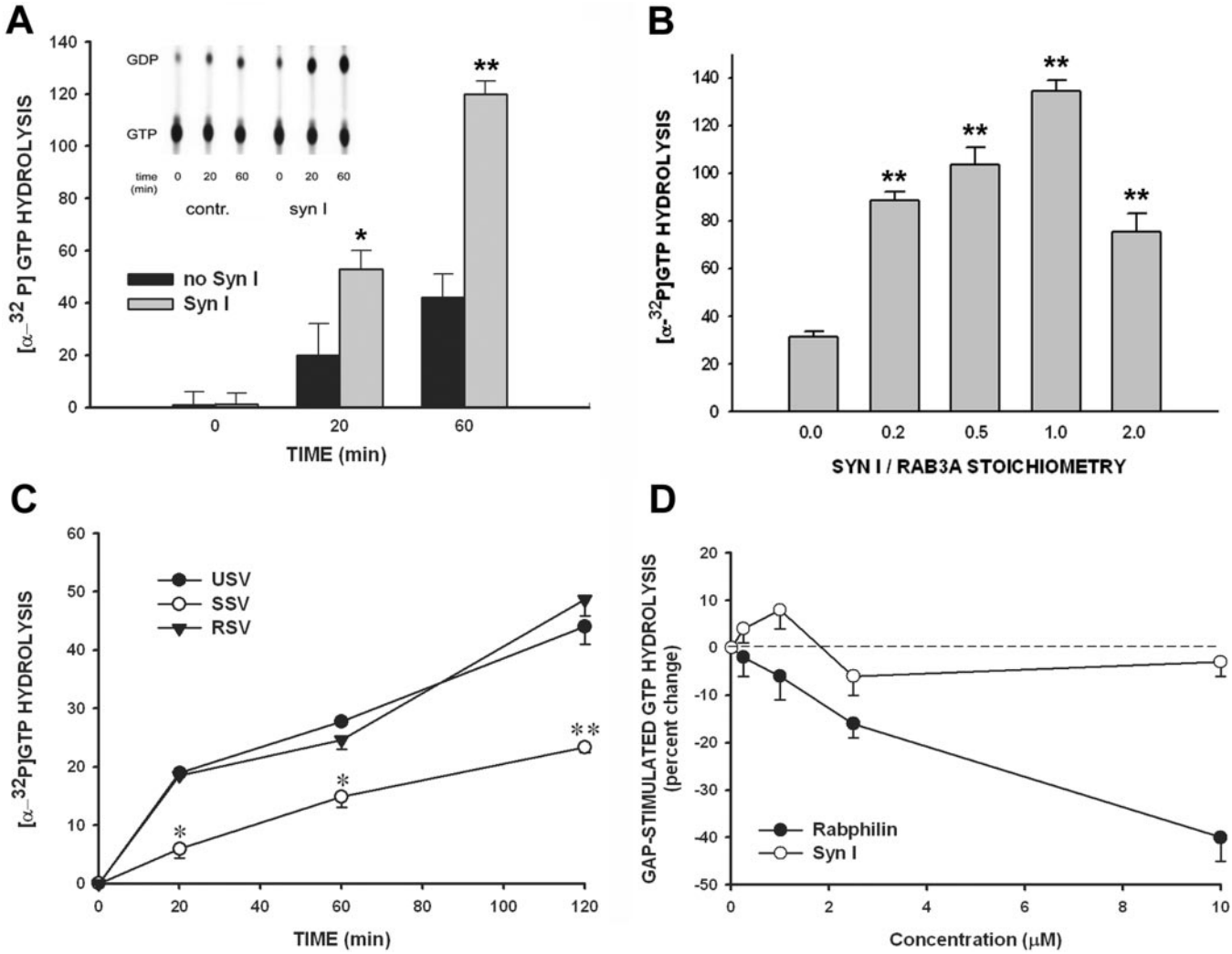

FIG. 1. **Synapsin I stimulates the GTPase activity of Rab3A.** *A*, purified [α-^{32}P]GTP-loaded Rab3A (25 pmol) was incubated at 30 °C for the indicated times in the absence (*black bars*) or presence (*gray bars*) of purified synapsin I (*Syn I*; 25 pmol). GTP hydrolysis was evaluated by TLC (*inset*) and expressed as percent increase in [α-^{32}P]GDP formation *versus* time 0 (means ± S.E.; $n = 5$). *, $p < 0.05$; **, $p < 0.01$, Student's *t* test *versus* Rab3A alone. *contr.*, control. *B*, dose-dependent effect of synapsin I on Rab3A GTPase activity. Purified [α-^{32}P]GTP-loaded Rab3A (25 pmol) was incubated for 60 min at 30 °C in the absence or presence of increasing amounts of purified synapsin I. GTP hydrolysis was evaluated as described in *A*. *Columns* in the plot are means ± S.E. ($n = 5$). **, $p < 0.01$, Duncan's multiple comparison test *versus* Rab3A alone. *C*, the endogenous GTPase activity associated with SV is regulated by synapsin I. Five micrograms of untreated SV (*black circles*), synapsin I-depleted SV (*white circles*), or synapsin I rebound SV (*black triangles*) were loaded with [α-^{32}P]GTP and incubated at 30 °C. Aliquots were taken at various times (20–120 min) and analyzed for GTP hydrolysis by TLC (see *A*). *Points* in the plot are means ± S.E. ($n = 5$). *, $p < 0.05$; **, $p < 0.01$, Duncan's multiple comparison test *versus* GTP hydrolysis in USV. *D*, effects of synapsin I and Rabphilin-3 on Rab3A-GAP activity. Purified [γ-^{32}P]GTP-loaded Rab3A (10 pmol) was incubated with recombinant Rab3A-GAP for 6 min at room temperature in the absence (control) or presence of either Rabphilin-3 (*black symbols*) or synapsin I (*white symbols*). Samples were filtered through cellulose filters, and the retained radioactivity linked to GTP was determined by scintillation counting. Data are expressed as percent changes with respect to the control samples (means ± S.E.; $n = 5$).

centrifugation in a Beckman TLA-100 rotor (400,000 × *g* for 30 min) for recovery of total F-actin (33). The actin pellets and supernatant fractions were solubilized in Laemmli sample buffer and subjected to SDS-PAGE (34). The amounts of actin in the various fractions were detected by Coomassie Blue staining, whereas the amounts of synapsin I bound to actin or free in the supernatant were determined by either protein staining of the gels or immunoblotting. Quantitative analysis of Coomassie-stained gels or immunoblots was performed either by laser scanning densitometry (Ultroscan XL, Amersham Biosciences) by interpolation of the density values into a suitable standard curve.

Vesicle Aggregation Assays—Phospholipid vesicles mimicking the phospholipid composition of SV (PC:PE:PS:PI:cholesterol = 40:32:12:5:10) or PC vesicles (PC:cholesterol = 90:10) were made by sonication as described previously (35). Fluorescently labeled vesicles had the same lipid composition with the addition of the appropriate amounts (2% of the total lipid, w/w) of NBD-PE or LRh-PE either alone (single-labeled liposomes) or in combination (double-labeled liposomes). Changes in synapsin-induced vesicle aggregation in the presence of either Rab3A-GDP or Rab3A-GTP were followed by analyzing the fluorescence resonance energy transfer (FRET) between the energy donor NBD-PE and the acceptor LRh-PE (35). Synapsin I (100 nM)-induced aggregation in the presence or absence of GDP- or GTP-bound Rab3A (1 μM) was followed by monitoring FRET at 22 °C using a PerkinElmer Life Sciences LS-50 spectrofluorometer according to two distinct assays. In the first case (aggregation/fusion assay), the fluorescence donor and acceptor were incorporated into separate vesicle populations. Two populations of vesicles (100 μg of phospholipid for each vesicle population, containing 2% labeled phospholipid) were mixed, and FRET was measured by exciting the donor at 470 nm and following either the decrease in NBD emission at 520 nm (NBD quenching) or the increase in LRh emission at 590 nm (excitation and emission slits of 2.5 and 5 nm, respectively). In the second assay (fusion assay), one population of vesicles containing both fluorophores in equimolar amounts (50 μg of phospholipid, 2% labeled phospholipids) was mixed with unlabeled vesicles (150 μg of phospholipid). Under these conditions, pure aggregation of vesicles not accompanied by fusion is silent *per se* but can by evaluated as an enhancement in the rate and extent of vesicle fusion induced by a subsequent addition of 3 mM Ca^{2+}. Membrane fusion, leading to intermixing of labeled and unlabeled membrane components, results in a decrease in the surface density of donor and acceptor

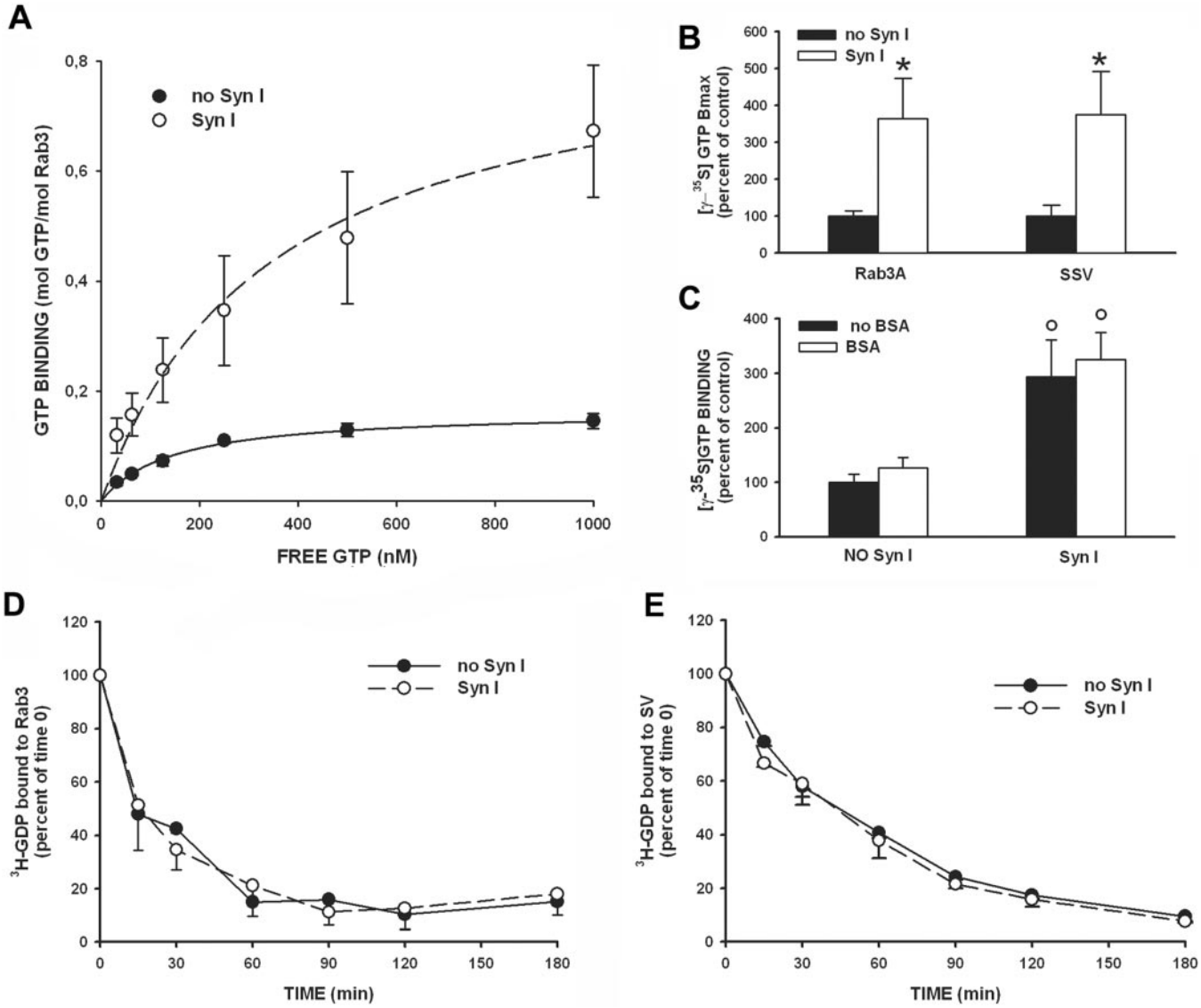

FIG. 2. **Synapsin I enhances GTP binding to Rab3A without affecting GDP dissociation.** *A* and *B*, GDP-loaded purified Rab3A (2 pmol) or synapsin I-depleted SV (10 μg) was incubated with increasing concentrations (30–1000 nM) of γ-^{35}S-GTP for 15 min at 30 °C in the absence (*black symbols* or *bars*) or presence (*white symbols* or *bars*) of 1 μM synapsin I (*Syn I*). Nonspecific binding was defined as the binding in the presence of an excess unlabeled GTP (300 μM). Incubation was stopped by rapid filtration on nitrocellulose filters, and the retained radioactivity was determined by liquid scintillation counting. The average binding isotherm of GTP binding to purified Rab3A, calculated according to the one ligand/one binding site model, is shown in *A*. *Points* in the plot represent means ± S.E. of six independent experiments. The calculated maximal GTP binding (B_{max}) to purified Rab3A or SSV is shown in *B* in percentage of the values observed in the absence of synapsin I (means ± S.E.; n = 6). *, $p < 0.01$, Student's t test *versus* control. *C*, the increase in GTP binding induced by synapsin I is not due to reversal of EDTA-induced Rab3A unfolding. GDP-loaded purified Rab3A was incubated with γ-^{35}S-GTP (1 μM) as described above in the absence (*black bars*) or presence (*white bars*) of BSA (2 mg/ml). Specific γ-^{35}S-GTP binding is expressed in percentage of the values observed in the absence of synapsin I and BSA (means ± S.E.; n = 4). °, $p < 0.01$; Student's t test *versus* samples incubated in the absence of synapsin I. No statistical difference was found between the two groups incubated in the absence or presence of BSA. *D* and *E*, recombinant Rab3A (2 pmol, *D*) or SSV (10 μg, *E*) were loaded with [^{3}H]GDP (1 μM) as described under "Experimental Procedures." GDP dissociation was triggered by an excess of GTP (300 μM) in the absence (*black symbols*) or presence (*white symbols*) of 1 μM synapsin I. The residual amount of [^{3}H]GDP bound to purified Rab3A or SSV was followed over time (15–180 min) and expressed in percent of the binding in the absence of GTP.

fluorophores and thereby in FRET that can be followed as an increase in NBD emission at 520 nm (NBD dequenching) or a decrease in LRh emission at 590 nm.

Rab3A-Synapsin I Pull-down Assays—The binding of glutathione *S*-transferase (GST)-Rab3A to dephosphorylated synapsin I or to synapsin I that had been stoichiometrically phosphorylated by either PKA, CaMKII, MAPK, or cdk-1 was assessed by co-precipitation experiments as follows. GST or GST-Rab3A loaded with GTPγS was coupled to glutathione-Sepharose (0.04 nmol of fusion protein per μl of settled beads) in binding buffer (10 mM Hepes, 150 mM NaCl, 1% (v/v) Triton X-100, 2 mg/ml BSA, pH 7.4) containing 5 mM $MgCl_2$. After extensive washing, protein-coupled beads (15 μl) were incubated with synapsin I (0.1–0.5 μM) in 500 μl of binding buffer for 3–5 h at 4 °C. After the incubation, the beads were pelleted by centrifugation, extensively washed with binding buffer and detergent-free binding buffer, resuspended in Laemmli sample buffer, and boiled for 2 min. Binding was analyzed by SDS-PAGE followed by quantitative immunoblotting.

Binding of Rab3A to Synaptic Vesicles

Purified SV containing endogenous synapsins (untreated SV (USV)) were quantitatively depleted of synapsin I by exposure to mild salt treatment (synapsin-depleted SV (SSV)) and reassociated *in vitro* with purified synapsin I (rebound SV (RSV)) as described previously (27). Purified SV (USV, SSV, or RSV, 20 μg protein/sample) were analyzed for the translocation of endogenous Rab3A and/or synapsin I between the SV-bound and the soluble form. SV were loaded with GDP or GTPγS (500 μM) in loading buffer for 15 min at 37 °C, chilled on ice, and supplemented with 20 mM $MgCl_2$ to stabilize the nucleotide-protein complex. Samples were then incubated for 45 min at 37 °C in the

presence of various concentrations of either synapsin I (0.25, 0.5, and 1 μM), purified RabGDI (0.05, 0.2, and 0.5 μM), or both. After the incubation, samples were centrifuged for 20 min at 450,000 × *g*, and the resulting supernatant and pellet fractions were analyzed by SDS-PAGE and immunoblotting.

RESULTS

Effects of Synapsin I on the Biochemical Properties of Rab3A—The rate of the Rab3 cycle within the nerve terminal is regulated by the key events of GDP/GTP exchange, which follows the association of Rab3 with SV, and GTP hydrolysis that promotes Rab3 dissociation from SV during priming and fusion. We employed biochemical assays to determine whether the association between synapsin I and Rab3 modulates Rab3 GTPase activity or nucleotide binding. The intrinsic Rab3 GTPase activity was assayed by measuring the decrease in the radioactivity associated with [α-^{32}P]GTP-loaded Rab3A and the corresponding increase in [α-^{32}P]GDP formation as a function of time. Synapsin I significantly stimulated the GTPase activity of both recombinant Rab3A (Fig. 1*A*) and endogenous Rab3 associated with highly purified SV (Fig. 1*C*). Synapsin I increased the GTPase activity of purified Rab3A in a time- and concentration-dependent manner, with a ≅5-fold increase in the initial rate of GTP hydrolysis at a 1:1 synapsin:Rab3A molar ratio (Fig. 1*B*). The GTPase activity of SV depleted of endogenous synapsin (SSV) was decreased by ~50% in comparison to untreated SV (USV), whereas the *in vitro* reassociation of purified synapsin I with synapsin depleted SV (RSV) restored GTP hydrolysis to the levels observed in untreated SV (Fig. 1*C*). Rabphilin, another SV Rab3 interactor stimulating Rab3 GTPase activity, is known to markedly inhibit in a dose-dependent fashion GAP-stimulated GTPase activity of Rab3 by binding to the Rab3 effector domain. However, at variance with Rabphilin-3, synapsin I did not inhibit the effect of GAP on Rab3 GTPase activity (Fig. 1*D*).

Equimolar concentrations of synapsin I significantly enhanced the binding of γ-^{35}S-GTP to both purified and SV-associated GDP-Rab3 by inducing a significant, 3-fold increase in the B_{max} of γ-^{35}S-GTP (Fig. 2, *A* and *B*). As the assay protocol involved nucleotide stripping by EDTA, we wondered whether the observed effects were simply attributable to Rab stabilization by a chaperone-like activity of synapsin I. To test this possibility, we repeated the assays in the presence of BSA and found that the effect of synapsin I was fully preserved also under these conditions (Fig. 2*C*), indicating that it was not merely due a nonspecific chaperone-like effect. At variance with GTP binding, the dissociation of [^{3}H]GDP from either recombinant Rab3A (Fig. 2*D*) or synapsin-depleted SV (Fig. 2*E*) triggered by an excess of GTP was not affected by the presence of synapsin I.

Modulation of the Synapsin-Rab3A Interaction by Synapsin Phosphorylation—Synapsin I is a target of multiple protein kinases, and site-specific phosphorylation of synapsin I is known to affect its interactions with SV and the actin cytoskeleton and its compartmentalization within nerve terminals (22, 36, 37). Thus, we evaluated whether phosphorylation of synapsin by either PKA (site 1), CaMKII (sites 2 and 3), MAPK (sites 4–6), or cdk-1 (site 6) was able to affect its interaction with Rab3A and the subsequent stimulation of Rab3A GTPase activity. Rab3A pull-down assays revealed that the interaction with synapsin I is poorly sensitive to its phosphorylation state, whereas phosphorylation by CaMKII was totally ineffective, phosphorylation by either PKA or MAPK/Erk induced only a mild decrease in the binding at low synapsin concentrations (Fig. 3*A*). Consistent with binding data, both phosphorylated and dephosphorylated forms of synapsin I significantly stimulated Rab3A GTPase activity, although PKA- or MAPK-phosphorylated synapsin I was less powerful than dephosphorylated synapsin I (Fig. 3*B*).

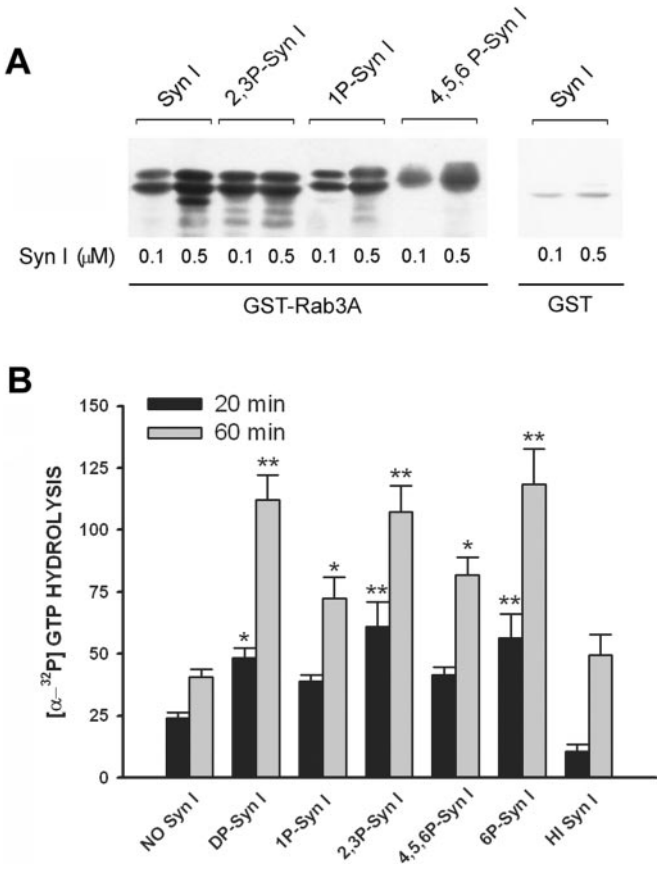

FIG. 3. **Effects of site-specific phosphorylation of synapsin I on the GTPase activity of Rab3A.** *A*, dephosphorylated synapsin I (*Syn I*) or synapsin I that had been stoichiometrically phosphorylated by either PKA on site 1 (*1P-Syn I*), by CaMKII on sites 2 and 3 (*2,3P-Syn I*), or by MAPK/Erk on sites 4–6 (*4,5,6P-Syn I*) was incubated with either GST or recombinant GST-Rab3A (20 μg) loaded with GTPγS, and the amounts of synapsin I bound to Rab3A were analyzed by quantitative immunoblotting. *B*, effects of site-specific phosphorylation of synapsin I on Rab3A-mediated GTP hydrolysis analyzed after 20 (*black bars*) or 60 min (*gray bars*) of incubation at 30 °C. The results are expressed as percent increase in [α-^{32}P]GDP formation *versus* time 0 (means ± S.E.; $n = 5$). *, $p < 0.05$; **, $p < 0.01$, Dunnett's multiple comparison test *versus* control (*NO Syn I*). For further details, see legend to Fig. 1. *6P-Syn I*, cdk1-phosphorylated synapsin I; *HI Syn I*, heat-inactivated synapsin I.

Effect of Rab3A on the Biochemical Properties of Synapsin I—Synapsin I binds to actin filaments via a major site located in the central domain C and induces the formation of actin bundles *in vitro* (33, 38). Thus, we investigated whether the interaction with Rab3A was able to interfere with the binding of synapsin I to F-actin and with the bundling of actin filaments induced by dephosphorylated synapsin I. Rab3A brought about a concentration-dependent inhibition of both synapsin binding to actin filaments and synapsin-induced actin bundling. Although the presence of up to 5 μM Rab3A did not alter actin assembly *per se*, it significantly inhibited the binding of synapsin I to F-actin and virtually abolished the synapsin I-induced actin filament bundling, as evaluated by high speed and low speed sedimentation assays, respectively (Fig. 4*A*). Analysis of the dose-response curves using a 3-parameter logistic function yielded IC_{50} values for actin bundling of 1.49 ± 0.16 and 1.31 ± 0.14 μM (means ± S.E.) for GDP-Rab3A and GTP-Rab3A, respectively, and IC_{50} values for synapsin binding to F-actin of 3.58 ± 0.28 and 3.14 ± 0.48 μM (means ± S.E.) for GDP-Rab3A and GTP-Rab3A, respectively. These values are in

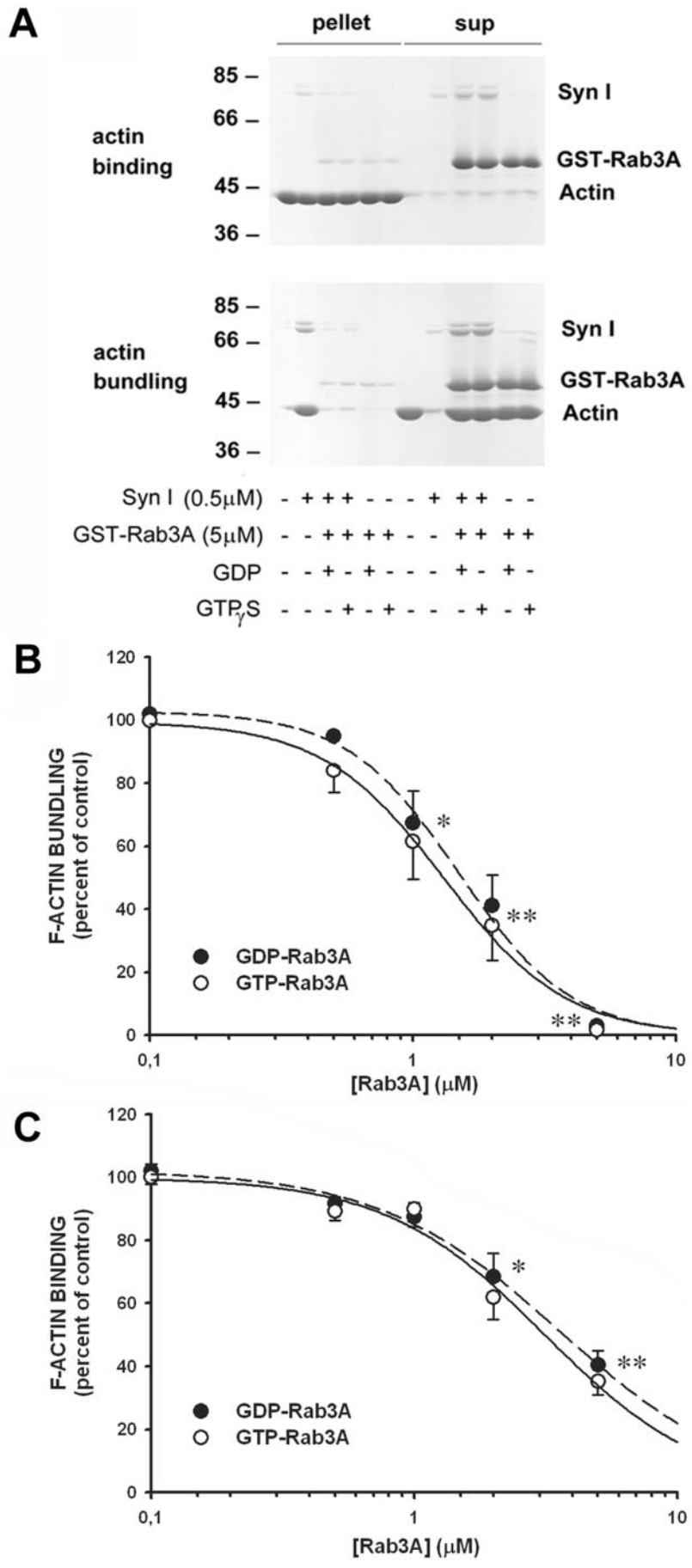

FIG. 4. **Rab3A inhibits the interactions of synapsin I with actin.** *A*, polymerized actin (5 μM) was incubated at room temperature for 1 h in the absence or presence of synapsin I (*Syn I*; 0.5 μM), Rab3A (5 μM), or both in the presence of either GTPγS or GDP. Identical samples were centrifuged at either low speed (10,000 $\times$ *g* for 10 min) for recovery of actin bundles (actin bundling) or high speed (400,000 $\times$ *g* for 30 min) for recovery of total F-actin (actin binding). Pellets and supernatant (*sup*) fractions were subjected to SDS-PAGE and analyzed by Coomassie Blue staining. No effects of the various treatments on the recovery of total F-actin were observed. No significant actin bundling was seen in the absence of synapsin I. *B* and *C*, the amounts of actin bundles (*B*) and of F-actin-bound synapsin I (*C*) recovered in the low and high speed pellets, respectively, were determined by densitometric scanning of the stained gels and of the synapsin immunoblots. The densitometric readings, expressed in percent of the respective values obtained in the control samples containing F-actin and synapsin alone, were plotted as means $\pm$ S.E. ($n = 5$) *versus* the concentration of GDP-Rab3A (*black symbols*) or GTP-Rab3A (*white symbols*). *, $p < 0.05$; **, $p < 0.01$, Dunnett's multiple comparison test *versus* control samples. Dose-response curves were analyzed using a 3-parameter logistic function. IC_{50} values for actin bundling were 1.49 $\pm$ 0.16 and 1.31 $\pm$ 0.14 μM (means $\pm$ S.E.) for GDP-Rab3A and GTP-Rab3A, respectively. IC_{50} values for synapsin I binding were 3.58 $\pm$ 0.28 and 3.14 $\pm$ 0.48 μM (means $\pm$ S.E.) for GDP-Rab3A and GTP-Rab3A, respectively.

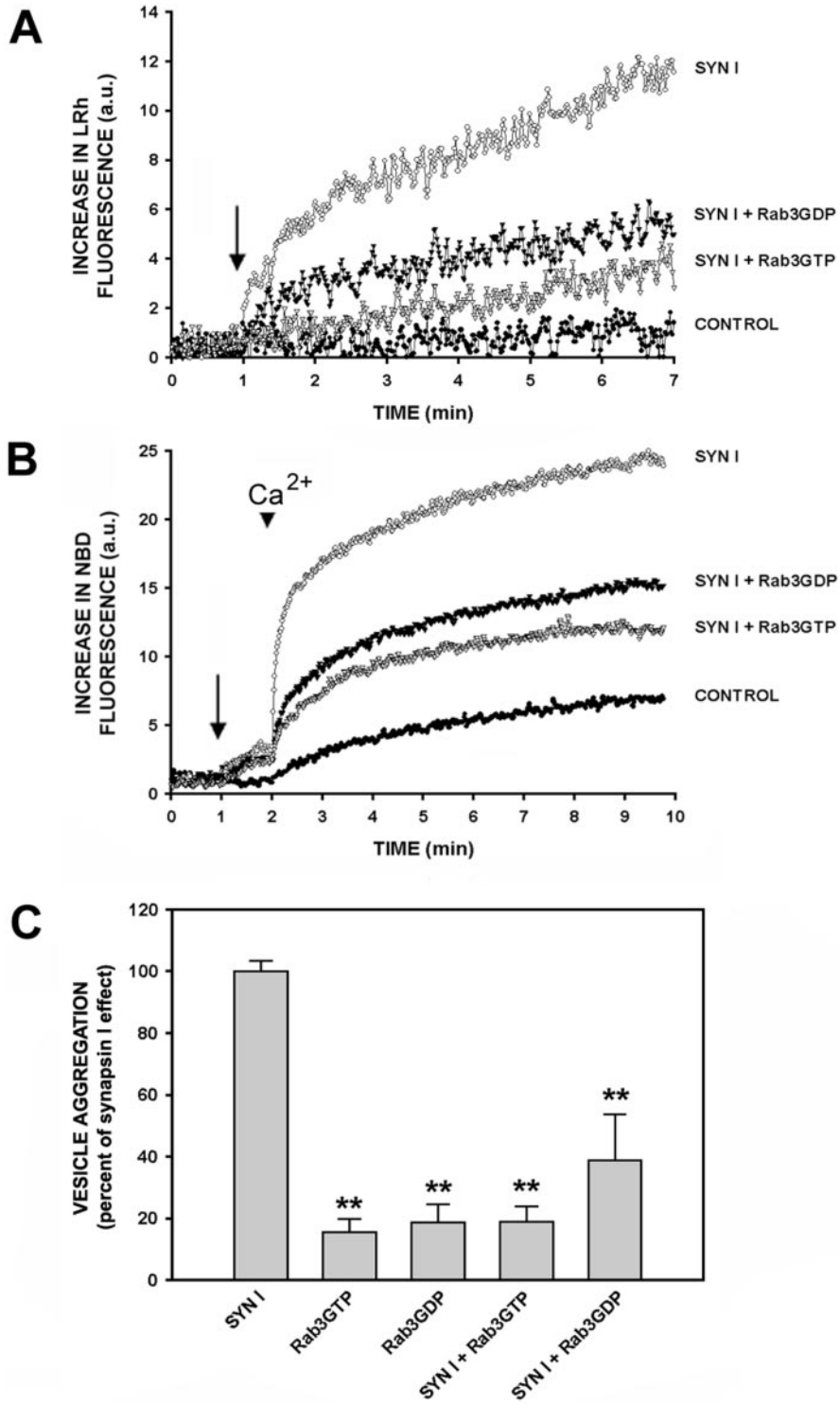

FIG. 5. **Rab3A inhibits the synapsin-induced phospholipid vesicle aggregation.** *A*, equal amounts of two populations of phospholipid vesicles mimicking the phospholipid composition of SV alternatively labeled with NBD-PE (donor) or LRh-PE (acceptor) were incubated (*arrow*) in the absence or presence of synapsin I (100 nM), GTP-, or GDP-loaded Rab3A (1 μM) or synapsin I plus Rab3A, and the FRET was followed as a function of time as the increase in the acceptor fluorescence (aggregation/fusion assay; see "Experimental Procedures"). FRET in the presence of Rab3A alone, either in the GDP- or GTP-bound form, did not differ from FRET under control conditions (not shown). *B*, phospholipid vesicles labeled with both NBD-PE and LRh-PE were mixed with unlabeled vesicles and preincubated for 1 min in the absence or presence of synapsin I (100 nM), GTP-, or GDP-loaded Rab3A (1 μM) or synapsin I plus Rab3A (*arrow*) before the addition of 3 mM $CaCl_2$ to trigger fusion (*arrowhead*). The decrease in FRET due to vesicle fusion was followed as a function of time as the increase in the donor fluorescence (fusion assay; see "Experimental Procedures"). *C*, for each experimental condition, the extent of FRET detected in the aggregation/fusion assay was determined 6 min after protein addition and plotted in percent of the FRET observed in the presence of synapsin I alone. **, $p < 0.01$ *versus* synapsin I alone; Duncan's multiple comparison test ($n = 5$).

good agreement with the estimated K_d of the synapsin-Rab3A binding (1–1.5 μM) (62). The physiological significance of this effect is also strengthened by taking into account the reduced accessibility of synapsin molecules engaged in the thick actin bundles and the observation that only 20% of recombinant Rab3A is nucleotide-bound after the loading procedure.

Synapsin I binds to phospholipid vesicles mimicking the phospholipid composition of SV, and its binding is associated with vesicle clustering and stabilization of the lipid bilayer (35). Thus, we investigated whether the association with Rab3A was able to interfere with the synapsin-induced vesicle clustering by using fluorometric assays sensitive to either vesicle aggregation or vesicle fusion (FRET aggregation/fusion assay) or specifically sensitive to fusion (FRET fusion assay; see "Experimental Procedures"). Both assays confirmed that synapsin I induces vesicle clustering without triggering fusion, as the addition of synapsin I readily increased FRET in the aggregation/fusion assay (Fig. 5*A*), whereas it only potentiated the fusogenic effect of a subsequent addition of Ca^{2+} in the fusion assay (Fig. 5*B*). Most interestingly, Rab3A in either the GDP- or GTP-bound form virtually abolished the synapsin I-induced aggregation of phospholipid vesicles (Fig. 5, *A–C*),

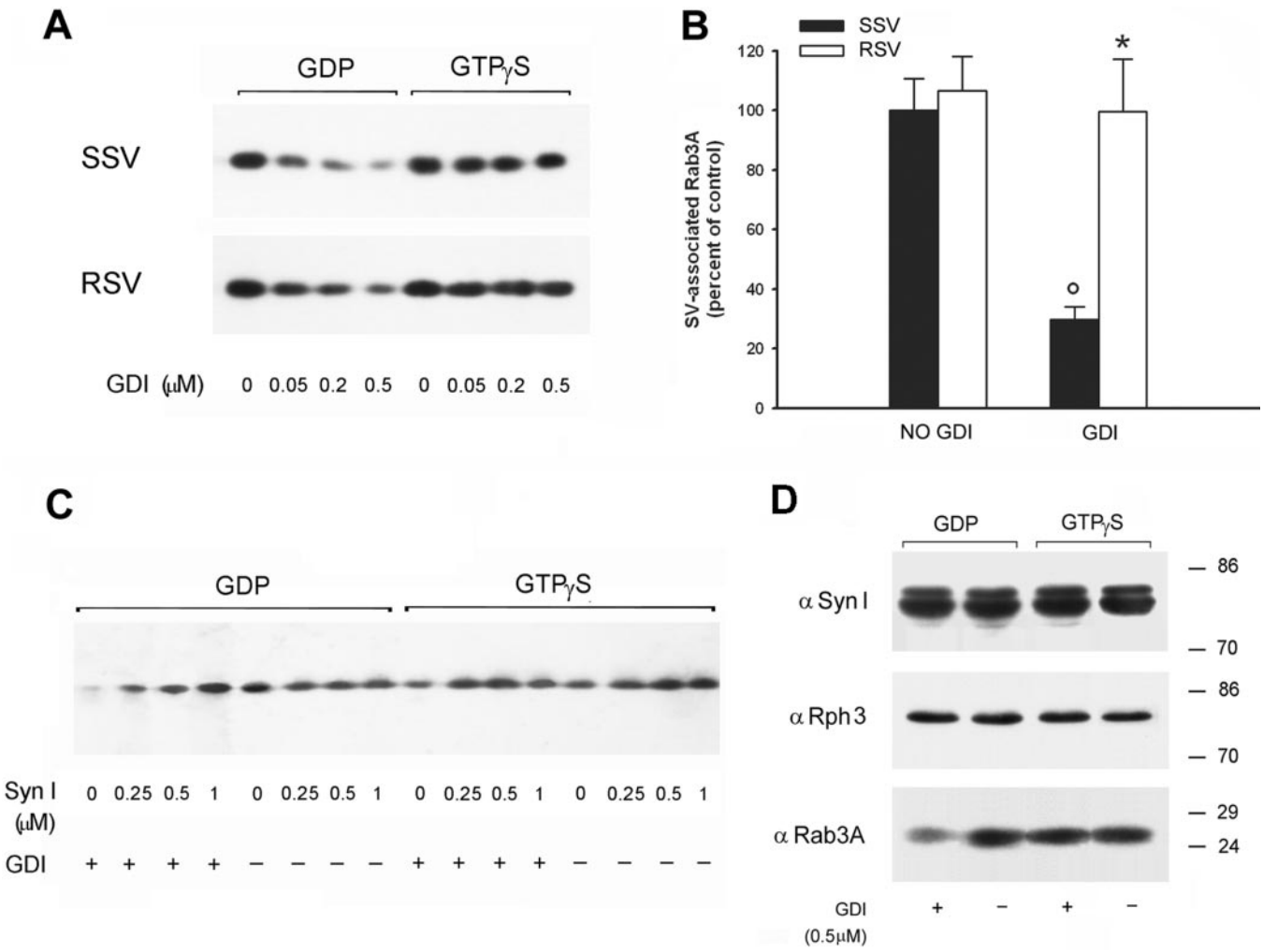

FIG. 6. **Synapsin I contributes to the association of Rab3A with synaptic vesicles.** *A*, highly purified SV depleted of endogenous synapsin I (SSV, 20 μg) or reassociated *in vitro* with purified synapsin I (rebound SV or RSV, 20 μg) and loaded with either GDP or GTPγS (500 μM) were incubated for 45 min at 37 °C in the presence of increasing concentrations of RabGDI and subjected to high speed centrifugation. The amount of Rab3A associated with the SV pellet was analyzed by immunoblotting with anti-Rab3A antibodies. *B*, the amount of Rab3A associated with synapsin-depleted SV (SSV, *black bars*) or with synapsin I-rebound SV (RSV, *white bars*) loaded with GDP and incubated in the absence or presence of RabGDI (0.5 μM) as described above was determined by quantitative immunoblotting. Data are expressed in percentage of the values observed in SSV in the absence of RabGDI (means ± S.E.; $n = 5$). *, $p < 0.01$ *versus* SSV in the presence of RabGDI; °, $p < 0.01$ *versus* SSV or RSV in the absence of RabGDI; Duncan's multiple comparison test. *C*, highly purified SV depleted of endogenous synapsin I (20 μg) loaded with either GDP or GTPγS (500 μM) were incubated for 45 min at 37 °C with increasing concentrations of synapsin I (*Syn I*; 0–1 μM) in the absence or presence of 0.5 μM RabGDI, and the amount of Rab3A associated with SV was analyzed as described in *A*. *D*, Rab3A does not contribute to the binding of synapsin I to SV. Untreated highly purified SV (20 μg) were incubated as described in *A* and simultaneously analyzed for the amounts of synapsin I, Rab3A, and Rabphilin-3 associated with the SV membrane by immunoblotting with anti-synapsin I (αSyn I), anti-Rabphilin-3 (αRph3), and anti-Rab3A (αRab3A) antibodies.

whereas it did not induce aggregation nor promote fusion when incubated with vesicle suspensions in the absence of synapsin I (Fig. 5*C*).

Effect of Synapsin I on the Association of Rab3A with Synaptic Vesicles—We next analyzed whether the synapsin-Rab3 interaction plays some role in the association of either Rab3A or synapsin I with the SV membrane. Incubation of purified SV with GDP and RabGDI removes Rab3A from the membrane, whereas the addition of the nonhydrolyzable GTP analogue GTPγS prevents Rab3A dissociation, consistent with the notion that RabGDI solubilizes Rab3A from SV following GTP hydrolysis (24, 39). To study whether synapsin I contributes to the association of Rab3A with SV, highly purified SV depleted of endogenous synapsin I or rebound to exogenous synapsin I at various degrees of saturation were analyzed for the translocation of Rab3A between the SV-bound and the soluble forms under conditions of GDP or GTPγS loading. RabGDI promoted a dose-dependent dissociation of Rab3A from synapsin-depleted SV (SSV) in the presence of GDP (but not of GTPγS) that was markedly decreased by the reassociation of synapsin I with the SV membrane (RSV; Fig. 6, *A* and *B*). For a given concentration of RabGDI, this effect was dependent on the degree of saturation of the SV membrane with synapsin I (Fig. 6*C*). As observed before, the effects of synapsin I were detectable only when Rab3A was in the GDP-bound form and in the presence of RabGDI. By preventing RabGDI-induced Rab3A solubilization, synapsin I might thus stabilize the association of Rab3A with SV. In contrast, Rab3A does not appear to contribute to the binding of synapsin I to SV. In fact, incubation of untreated SV containing endogenous synapsin I under conditions promoting Rab3A dissociation (GDP loading and RabGDI) did not significantly affect the association of synapsin I (or of the other SV-associated Rab3 effector Rabphilin 3) with the SV membrane (Fig. 6*D*).

The role of synapsin I in the subcellular compartmentalization of Rab3A was also analyzed in mutant mice lacking syn-

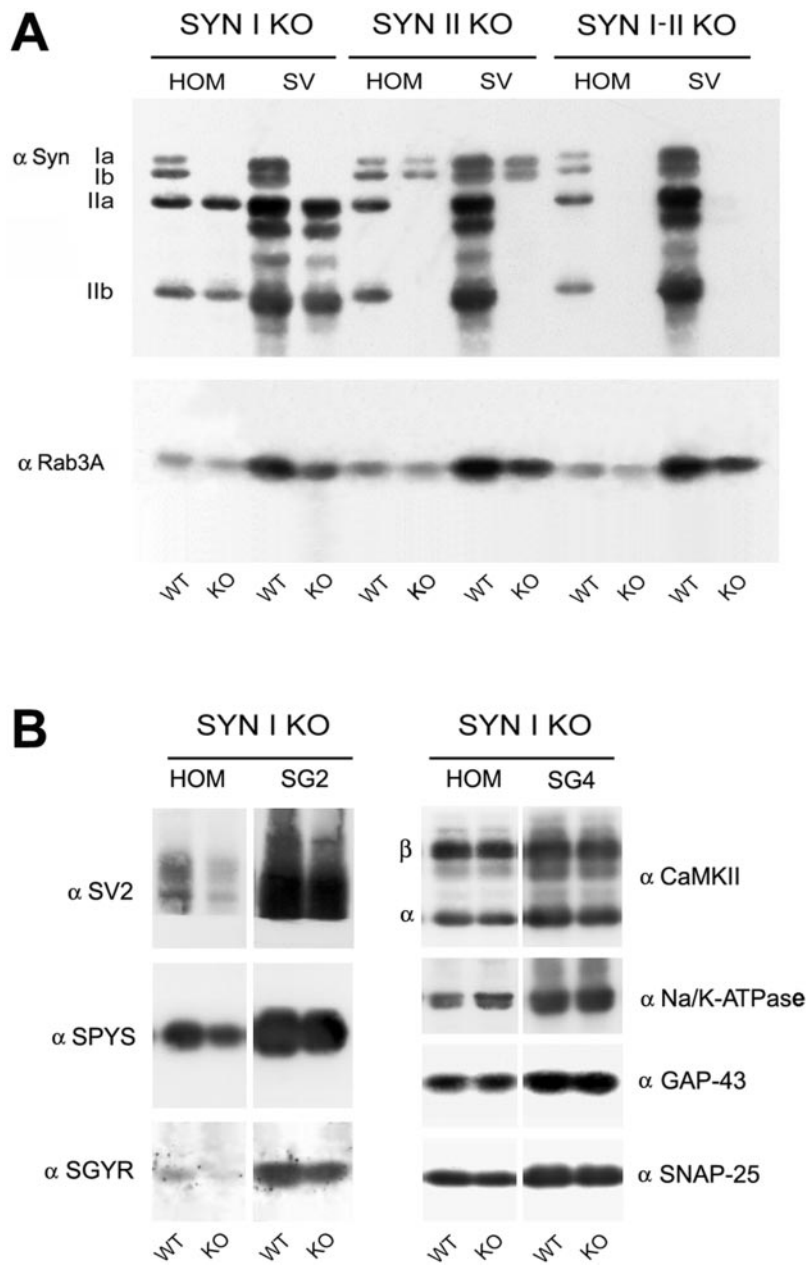

FIG. 7. **The amount of Rab3A associated with SV is decreased in synapsin I, synapsin II, and synapsin I/II knockout mice.** *A*, homogenate (*HOM*) and purified SV (SG2 fraction) obtained from synapsin I, synapsin II, and synapsin I/II knockout (*KO*) mice were analyzed by SDS-PAGE and immunoblotting with anti-synapsin (G143) and anti-Rab3A antibodies. *WT*, wild type. *B*, brain homogenate and fractions enriched in SV or synaptic membranes (SG2 and SG4 fractions, respectively) obtained from wild-type and synapsin I knockout mice were assayed for their content of the integral SV proteins SV2, synaptophysin (*SPYS*), and synaptogyrin (*SGYR*) (*left*) or of the synaptic membrane-associated proteins CaMKII, Na/K-ATPase, GAP-43, and SNAP-25 (*right*) by immunoblotting with specific antibodies.

apsin I, synapsin II, or both. Whereas the expression levels of Rab3A in total brain homogenate were not greatly affected in mutant animals, as reported previously (40), the levels of Rab3A associated with sucrose gradient-purified SV (SG2 fraction) were markedly decreased in synapsin knockout mice with respect to wild-type littermates (Fig. 7*A*), suggesting that the association with synapsin participates in the correct targeting of Rab3A to the SV compartment. At variance with Rab3A, in synapsin I knockout mice the levels of other integral SV proteins such as SV2, synaptophysin, or synaptogyrin were decreased in both brain homogenate and purified SV to approximately the same extent, reflecting the decreased number of SV observed in these animals (40, 41), whereas other proteins predominantly associated with synaptic membranes, such as CaMKII, Na^+/K^+-ATPase, GAP-43, or SNAP-25, were not affected in both the homogenate and a sucrose gradient fraction (SG4) enriched in synaptic membranes (Fig. 7*B*).

DISCUSSION

We have shown recently that Rab3A, the most abundant monomeric GTPase associated with SV and involved in the regulation of the exo-endocytotic cycle of SV, interacts with synapsin I in purified SV and intact nerve terminals (62). Synapsins have also been implicated in the regulation of SV trafficking (35–37, 42, 43) and of the kinetics of the final steps that immediately precede exocytotic fusion (23, 24). As shown in Fig. 8, both proteins cycle between a cytosolic and an SV-associated form and may represent clocks for the SV cycle by ensuring directionality and reversibility to the process. Thus, the interaction between synapsin I and Rab3A can be potentially involved in various stages of the SV cycle.

The formation of a complex between synapsin I and Rab3A affects the biochemical properties of both proteins. Synapsin I enhances the intrinsic GTPase activity of Rab3A and the binding of GTP to GDP-Rab3A, suggesting that it can act as a positive modulator of the Rab3A cycle. As synapsin I does not affect GDP dissociation from either purified or SV-associated Rab3A, the increase in GTP binding to Rab3A is likely to be attributable to a conformational effect that makes Rab3A more suitable for GTP binding. When compared with Rab3GAP, synapsin I induces a rather weak stimulation of GTP hydroly-

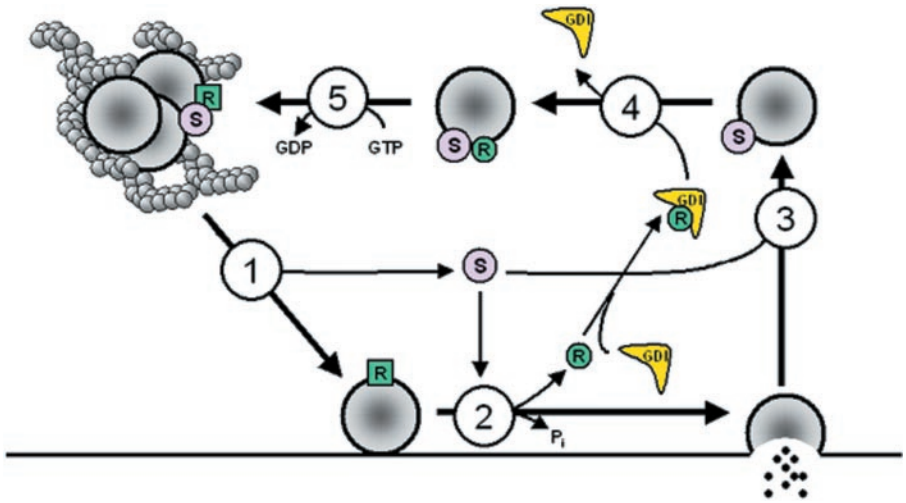

FIG. 8. **Putative role of synapsin I-Rab3A in the exo-endocytotic cycle of synaptic vesicles.** Evoked neurotransmitter release is a multistep process in which SV, after being released from the actin cytoskeleton (*step 1*), dock to presynaptic membrane and undergo the sequential steps of priming and Ca^{2+}-triggered fusion (*step 2*). After fusion, SV are retrieved through a process of endocytosis (*step 3*) and become competent for a new round of exocytosis (*steps 4* and *5*). Both synapsin I (*S*) and Rab3A (*R*) cycle between a cytosolic and an SV-associated form. Synapsin I partially dissociates from SV and actin during step 1, making SV available for exocytosis, increases the rate of the post-docking events of priming and/or fusion (*step 2*), and reassociates with SV after endocytosis (*step 3*). On the other hand, GTP-Rab3A (*green square*) is bound to SV through an association with SV effectors such as synapsin I and Rabphilin-3 (not shown). After docking, membrane-bound GTP-Rab3A negatively modulates priming/fusion and eventually dissociates from the SV membrane upon GTP hydrolysis by the action of GDI (*step 2*). After endocytosis, GDP-Rab3 (*green circle*) is delivered to SV where it binds to synapsin I (*step 4*) and undergoes GTP/GDP exchange (*step 5*) to reenter the cycle. The interaction between synapsin I and Rab3 may function in (i) accelerating priming/fusion by stimulation of GTP hydrolysis (*step 2*); (ii) promoting the recruitment of GDP-Rab3A from the soluble RabGDI-associated store to the SV membrane (*step 4*) and the subsequent GTP/GDP exchange (*step 5*); and (iii) increasing SV availability for release (*step 1*) by inhibiting the actin binding and SV clustering activities of synapsin I.

sis possibly by stabilizing the switch regions of Rab3A, as already reported for Rabphilin-3 (44). However, at variance with Rabphilin-3, the stimulation of GTP hydrolysis by synapsin I is not mutually exclusive with that promoted by Rab3GAP, and the possibility exists that basic residues in the COOH-terminal region of synapsin I involved in Rab3A binding (syn-(618–652)) bind to the γ-phosphate of GTP, mimicking the Rab3GAP arginine finger (31).

It is of interest to compare the respective properties of Rabphilin-3 and synapsin I, the two major SV-associated Rab3 effector proteins. Both proteins are extrinsic membrane proteins that bind SV through multiple sites (21, 46, 50), display phospholipid binding, are phosphorylated by Ca^{2+}-dependent kinases that regulate their SV association, interact with actin or actin-binding proteins, bind to the Rab3 effector domain, and promote a weak stimulation of Rab3 GTPase activity (16, 21, 22, 44–47). Most interestingly, Rab3A binding inhibits both the interaction of Rabphilin-3 with α-actinin, an actin filament cross-linking protein (16), and the binding/bundling of actin filaments by synapsin I (this paper), indicating a role of these interactions in the activity-dependent reorganization of the actin cytoskeleton of the nerve terminal. However, important differences exist. Rabphilin-3 displays a higher binding affinity for Rab3A than synapsin I (48, 49), and its binding is entirely specific for the GTP-bound form of Rab3A and strongly inhibits Rab3-GAP activity (31, 44), which is not the case for synapsin I binding. Although conflicting results were reported on whether Rabphilin-3 recruits GTP-Rab3A to SV or is recruited to SV by GTP-Rab3 (17, 51), it has been shown that the GDP-bound form of Rab3A associates with SV before GTP/GDP exchange (18) (Fig. 8, *steps 4* and *5*) and that synapsin I may play a role both in recruiting GDP-Rab3A to SV and in the subsequent GTP binding to Rab3A (this paper). Accordingly, no changes in Rab3A compartmentalization have been observed in Rabphilin-3 knockout mice (52), whereas a decreased SV targeting of Rab3A is present in mutant mice lacking synapsins (this paper). These observations suggest that synapsin I and Rabphilin-3 can operate in series as it often occurs for Rab effectors, with synapsin binding to Rab3A preceding Rabphilin-3 binding to the SV membrane.

It is not yet clear whether GTP hydrolysis is important for Rab3A to accomplish its function and the precise step at which Rab3A acts. However, a large body of experimental data indicate that GTP-bound Rab3A interacts with a prefusion complex preventing fusion and that GTP hydrolysis removes this inhibition (for review see Refs. 2, 4, and 53) (Fig. 8, *step 2*). Indeed, in a variety of experimental systems overexpression of constitutively active Rab3A inhibits neurotransmitter release (8–10), whereas mutant mice lacking Rab3A exhibit an increased number of SV fusion events per synapse and per impulse, suggesting a role of Rab3A in regulating the efficiency of the priming and/or fusion step(s) (13). Thus, it is tempting to speculate that the role of synapsin I in determining the kinetics of SV fusion (23, 24) (Fig. 8, *step 2*) is linked to its interaction with Rab3A.

Recent work has indicated that the reassociation of Rab3A with SV after endocytosis occurs through delivery of GDP-Rab3A to SV by RabGDI and involves a protein component of SV that is not Rabphilin-3 (17, 18) (Fig. 8, *step 4*). Indeed, synapsin I increases the association of GDP-Rab3A with the SV membrane in the presence of RabGDI. This effect indicates that synapsin I competes with RabGDI for GDP-Rab3A, exhibiting a GDI dissociation factor-like activity (19, 20). This interpretation is strengthened by the following observations. (i) Synapsin I can bind also to GDP-Rab3A, although to a lesser extent than to GTP-Rab3A (62). (ii) Rab3A recruitment by SV in the presence of RabGDI parallels the amount of synapsin I bound to SV. (iii) In genetically altered mice lacking synapsins, Rab3A appears to be mistargeted, as the amount of Rab3A associated with SV is decreased, whereas the total amount of Rab3A in brain is not significantly affected (Ref. 40 and this paper).

The engagement of synapsin I in Rab3A binding alters its interactions with actin and SV by inhibiting F-actin binding, actin bundle formation, and vesicle clustering. As both the bundling of F-actin and the phospholipid vesicle aggregation

induced by synapsin I are likely to be contributed by self-association of synapsin molecules (35, 38, 54, 55) each binding to single actin filaments or to phospholipid membranes, it is tempting to speculate that the effect of Rab3A on synapsin-induced actin filament bundling and vesicle aggregation is attributable to a change in the dimerization properties of synapsin I. Indeed, preliminary data revealed that equimolar concentrations of Rab3A markedly inhibit synapsin I dimerization.[2]

The Rab3A-induced changes in synapsin function may alter the maintenance of the reserve pool of SV by reducing recruitment of SV in the actin-bound clusters and increasing their availability for exocytosis (22, 36, 37, 43) (Fig. 8, *step 1*). Indeed, Rab3A knockout mice also exhibited a decrease in the activity-dependent recruitment of SV to the active zone and an incomplete recovery of the secretory response after exhaustive stimulation (15). These effects, which become apparent under conditions of high frequency stimulation and high probability of release, are qualitatively similar to those observed in synapsin knockout mice and *Aplysia* neurons after synapsin neutralization (24, 40, 41). A large body of experimental evidence indicates that Rab GTPases, such as Rab6, Rab7, Rab11, or Rab27, regulate intracellular vesicle trafficking by mediating the interactions between organelles and the cytoskeleton (56–61). The data presented here indicate that also Rab3A, by interacting with synapsin I and modulating its actin binding activity, can participate in the control of SV trafficking within nerve terminals.

In conclusion, we have demonstrated that synapsin I is a novel Rab3A effector. As shown in Fig. 8, this interaction may function in accelerating the rate of the Rab3A cycle at multiple levels by facilitating GTP hydrolysis (*step 2*), GDP-Rab3A reassociation with recycled SV (*step 4*), and GTP binding (*step 5*) as well as in promoting an increased availability of SV for exocytosis by down-regulating the pre-docking functions of synapsin I (*step 1*). Further functional studies are required to define in more detail the functional implications of the synapsin-Rab3A interaction in the fine-tuning of the exo-endocytotic cycle of SV and in the regulation of the efficiency and kinetics of neurotransmitter release.

Acknowledgments—We thank Dr. W. E. Balch (Scripps Research Institute, La Jolla, CA) for the generous gifts of the rat RabGDI construct and Dr. G. Cesareni for critical reading of the manuscript.

REFERENCES

1. Zerial, M., and McBride, H. (2001) *Nat. Rev. Mol. Cell Biol.* **2,** 107–117
2. Takai, Y., Sasaki, T., and Matozaki, T. (2001) *Physiol. Rev.* **81,** 153–208
3. Schluter, O. M., Khvotchev, M., Jahn, R., and Südhof, T. C. (2002) *J. Biol. Chem.* **277,** 40919–40929
4. Geppert, M., and Südhof, T. C. (1998) *Annu. Rev. Neurosci.* **21,** 75–95
5. Jahn, R., Lang, T., and Südhof, T. C. (2003) *Cell* **112,** 519–533
6. Fischer von Mollard, G., Südhof, T. C., and Jahn, R. (1991) *Nature* **349,** 79–81
7. Fischer von Mollard, G., Stahl, B., Khokhlatchev, A., Südhof, T. C., and Jahn, R. (1994) *J. Biol. Chem.* **269,** 10971–10974
8. Johannes, L., Lledo, P.-M., Roa, M., Vincent, J.-D., Henry, J.-P., and Darchen, F. (1994) *EMBO J.* **13,** 2029–2037
9. Johannes, L., Dousseau, F., Clabecq, A., Henry, J.-P., Darchen, F., and Poulain, B. (1996) *J. Cell Sci.* **109,** 2875–2884
10. Dousseau, F., Clabecq, A., Henry, J.-P., Darchen, F., and Poulain, B. (1998) *J. Neurosci.* **18,** 3147–3157
11. Wang, Y., Okamoto, M., Schimtz, F., Hofmann, K., and Südhof, T. C. (1997) *Nature* **388,** 593–598
12. Gonzales, L., and Scheller, R. H. (1999) *Cell* **96,** 755–758
13. Geppert, M., Goda, Y., Stevens, C. F., and Südhof, T. C. (1997) *Nature* **387,** 810–814
14. Koushika, S. P., Richmon, J. E., Hadwiger, G., Weimer, R. M., Jorgensen, E. M., and Nonet, M. L. (2001) *Nat. Neurosci.* **4,** 997–1005
15. Leenders, A. G., Lopes da Silva, F. H., Ghijsen, W. E., and Verhage, M. (2001) *Mol. Biol. Cell* **12,** 3095–3102
16. Kato, M., Sasaki, T., Ohya, T., Nakanishi, H., Nishioka, H., Imamura, M., and Takai, Y. (1996) *J. Biol. Chem.* **271,** 31775–31778
17. Stahl, B., Chou, J. H., Li, C., Südhof, T. C., and Jahn, R. (1996) *EMBO J.* **15,** 1799–1809
18. Chou, J. H., and Jahn, R. (2000) *J. Biol. Chem.* **275,** 9433–9440
19. Dirac-Svejstrup, A. B., Sumizawa, T., and Pfeffer, S. R. (1997) *EMBO J.* **16,** 465–472
20. Sivars, U., Aivazian, D., and Pfeffer, S. R. (2003) *Nature* **425,** 856–859
21. Greengard, P., Valtorta, F., Czernik, A. J., and Benfenati, F. (1993) *Science* **259,** 780–785
22. Hilfiker, S., Pieribone, V. A., Czernik, A. J., Kao, H. T., Augustine, G. J., and Greengard, P. (1999) *Philos. Trans. R. Soc. Lond. B Biol. Sci.* **354,** 269–279
23. Hilfiker, S., Schweizer, F. E., Kao, H. T., Czernik, A. J., Greengard, P., and Augustine, G. J. (1998) *Nat. Neurosci.* **1,** 29–35
24. Humeau, Y., Dousseau, F., Vitiello, F., Greengard, P., Benfenati, F., and Poulain, B. (2001) *J. Neurosci.* **21,** 4195–4206
25. Schiebler, W., Jahn, R., Doucet, J.-P., Rothlein, J., and Greengard, P. (1986) *J. Biol. Chem.* **261,** 8383–8390
26. Jovanovic, J. N., Benfenati, F., Siow, Y. L., Sihra, T. S., Sanghera, J. S., Pelech, S. L., Greengard, P., and Czernik, A. J. (1996) *Proc. Natl. Acad. Sci. U. S. A.* **93,** 3679–3683
27. Huttner, W. B., Schiebler, W., Greengard, P., and De Camilli, P. (1983) *J. Cell Biol.* **96,** 1374–1388
28. Kikuchi, A., Nakanishi, H., and Takai, Y. (1995) *Methods Enzymol.* **257,** 57–70
29. Burstein, E. S., Linko-Stentz, K., Lu, Z., and Macara, I. G. (1991) *J. Biol. Chem.* **266,** 2689–2692
30. Bochner, B. R., and Ames, B. N. (1982) *J. Biol. Chem.* **257,** 9759–9769
31. Clabecq, A., Henry, J.-P., and Darchen, F. (2000) *J. Biol. Chem.* **275,** 31786–31791
32. Benfenati, F., Valtorta, F., Chieregatti, E., and Greengard, P. (1992) *Neuron* **8,** 377–386
33. Bähler, M., and Greengard, P. (1987) *Nature* **326,** 704–707
34. Laemmli, U. K. (1970) *Nature* **227,** 680–685
35. Benfenati, F., Valtorta, F., Rossi, M. C., Onofri, F., Sihra, T., and Greengard, P. (1993) *J. Cell Biol.* **123,** 1845–1855
36. Chi, P., Greengard, P., and Ryan, T. A. (2001) *Nat. Neurosci.* **4,** 1187–1193
37. Chi, P., Greengard, P., and Ryan, T. A. (2003) *Neuron* **10,** 69–78
38. Bähler, M., Benfenati, F., Valtorta, F., Czernik, A. J., and Greengard, P. (1989) *J. Cell Biol.* **108,** 1841–1849
39. Araki, S., Kikuchi, A., Hata, Y., Isoaura, M., and Takai, Y. (1990) *J. Biol. Chem.* **265,** 13007–13025
40. Rosahl, T. W., Spillane, D., Missler, M., Herz, J., Selig, D. K., Wolff, J. R., Hammer, R. E., Malenka, R. C., and Südhof, T. C. (1995) *Nature* **375,** 488–493
41. Li, L., Chin, L.-S., Shupliakov, O., Brodin, L., Sihra, T. S., Hvalby, Ø., Jensen, V., Zheng, D., McNamara, J. O., Greengard, P., and Andersen, P. (1995) *Proc. Natl. Acad. Sci. U. S. A.* **92,** 9235–9239
42. Ceccaldi, P., Grohovaz, F., Benfenati, F., Chieregatti, E., Greengard, P., and Valtorta, F. (1995) *J. Cell Biol.* **128,** 905–912
43. Bloom, O., Evergren, E., Tomilin, N., Kjaerulff, O., Low, P., Brodin, L., Pieribone, V. A., Greengard, P., and Shupliakov, O. (2003) *J. Cell Biol.* **161,** 737–747
44. Kishida, S., Shiritaki, H., Sasaki, T., Kato, M., Kaibuchi, K., and Takai, Y. (1993) *J. Biol. Chem.* **268,** 22259–22261
45. Fykse, E. M., Li, C., and Südhof, T. C. (1995) *J. Neurosci.* **15,** 2385–2395
46. Senbonmatsu, T., Shirataki, H., Jin-No, Y., Yamamoto, T., and Takai, Y. (1996) *Biochem. Biophys. Res. Commun.* **228,** 567–572
47. Folletti, D. L., Blitzer, J. T., and Scheller, R. H. (2001) *J. Neurosci.* **21,** 5473–5483
48. Chung, S.-H., Yoberty, G., Gelino, E. A., Macara, I. G., and Holz, R. W. (1999) *J. Biol. Chem.* **274,** 18113–18120
49. Wang, X., Hu, B., Zimmermann, B., and Kilimann, M. W. (2001) *J. Biol. Chem.* **276,** 32480–32488
50. Shirataki, H., Kaibuchi, K., Sadoka, T., Kishida, S., Yamaguchi, T., Wada, K., Miyazaki, M., and Takai, Y. (1993) *Mol. Cell. Biol.* **13,** 2061–2068
51. Shirataki, H., Yamamoto, T., Hagi, S., Miura, H., Oishi, H., Jin-No, J., Senbonmatsu, T., and Takai, Y. (1994) *J. Biol. Chem.* **269,** 32717–32720
52. Schlüter, O. M., Schnell, E., Verhage, M., Tzonopoulos, T., Nicoll, R.A., Janz, R., Malenka, R., Geppert, M., and Südhof, T. C. (1999) *J. Neurosci.* **19,** 5834–5846
53. Darchen, F., and Goud, B. (2000) *Biochimie* (*Paris*) **82,** 375–384
54. Hosaka, M., and Südhof, T. C. (1999) *J. Biol. Chem.* **274,** 16747–17653
55. Cheetham, J. J., Hilfiker, S., Benfenati, F., Weber, T., Greengard, P., and Czernik, A. J. (2001) *Biochem. J.* **354,** 57–66
56. Echard, A., Jollivet, F., Martinez, O., Lacapere, J. J., Rousselet, A., Janoueix-Lerosey, I., and Goud, B. (1998) *Science* **279,** 580–585
57. Jordens, I., Fernandez-Borja, M., Marsman, M., Dusseljee, S., Janssen, L., Calafat, J., Janssen, H., Wubbolts, R., and Neefjes, J. (2001) *Curr. Biol.* **11,** 1680–1685
58. Hales, C. M., Vaerman, J. P., and Goldenring, J. R. (2002) *J. Biol. Chem.* **277,** 50415–50421
59. Waselle, L., Coppola, T., Fukuda, M., Iezzi, M., El-Amraoui, A., Petit, C., and Regazzi, R. (2003) *Mol. Biol. Cell* **14,** 4103–4113
60. El-Amraoui, A., Schonn, J. S., Kussel-Andermann, P., Blanchard, S., Desnos, C., Henry, J. P., Wolfrum, U., Darchen, F., and Petit, C. (2002) *EMBO Rep.* **3,** 463–470
61. Desnos, C., Schonn, J. S., Huet, S., Tran, V. S., El-Amraoui, A., Raposo, G., Fanget, I., Chapuis, C., Menasche, G., de Saint Basile, G., Petit, C., Cribier, S., Henry, J. P., and Darchen, F. (2003) *J. Cell Biol.* **163,** 559–570
62. Giovedì S., Vaccaro P., Valtorta F., Darchen F., Greengard P., Cesareni G., and Benfenati F. (2004) *J. Biol. Chem.* **279,** 43760–43768

[2] S. Giovedì and F. Benfenati, unpublished results.

Synapsin Is a Novel Rab3 Effector Protein on Small Synaptic Vesicles: II. FUNCTIONAL EFFECTS OF THE Rab3A-SYNAPSIN I INTERACTION

Silvia Giovedì, François Darchen, Flavia Valtorta, Paul Greengard and Fabio Benfenati

J. Biol. Chem. 2004, 279:43769-43779.
doi: 10.1074/jbc.M404168200 originally published online July 20, 2004
